

# UC Berkeley

## UC Berkeley Previously Published Works

### Title

C-C Bond Cleavage Approach to Complex Terpenoids: Development of a Unified Total Synthesis of the Phomactins

### Permalink

<https://escholarship.org/uc/item/2qg126dm>

### Journal

Journal of the American Chemical Society, 142(36)

### ISSN

0002-7863

### Authors

Leger, Paul R  
Kuroda, Yusuke  
Chang, Stanley  
[et al.](#)

### Publication Date

2020-09-09

### DOI

10.1021/jacs.0c07316

Peer reviewed



Published in final edited form as:

*J Am Chem Soc.* 2020 September 09; 142(36): 15536–15547. doi:10.1021/jacs.0c07316.

## C–C Bond Cleavage Approach to Complex Terpenoids: Development of a Unified Total Synthesis of the Phomactins

**Paul R. Leger,**

Department of Chemistry, University of California, Berkeley, California 94720, United States

**Yusuke Kuroda,**

Department of Chemistry, University of California, Berkeley, California 94720, United States

**Stanley Chang,**

Department of Chemistry, University of California, Berkeley, California 94720, United States

**Justin Jurczyk,**

Department of Chemistry, University of California, Berkeley, California 94720, United States

**Richmond Sarpong**

Department of Chemistry, University of California, Berkeley, California 94720, United States

### Abstract

The rearrangement of carbon–carbon (C–C) single bonds in readily available carbocyclic scaffolds can yield uniquely substituted carbocycles that would be challenging to construct otherwise. This is a powerful and often non-intuitive approach for complex molecule synthesis. The transition-metal-mediated cleavage of C–C bonds has the potential to broaden the scope of this type of skeletal remodeling by providing orthogonal selectivities compared to more traditional pericyclic and carbocation-based rearrangements. To highlight this emerging technology, a unified, asymmetric, total synthesis of the phomactin terpenoids was developed, enabled by the selective C–C bond cleavage of hydroxylated pinene derivatives obtained from carvone. In this full account, the challenges, solutions, and intricacies of Rh(I)-catalyzed cyclobutanol C–C cleavage in a complex molecule setting are described. In addition, details of the evolution of strategies that ultimately led to the total synthesis of phomactins A, K, P, R, and T, as well as the synthesis and structural reassignment of Sch 49027, are given.

### Graphical Abstract

---

**Corresponding Author** rsarpong@berkeley.edu.

Notes

The authors declare no competing financial interest.

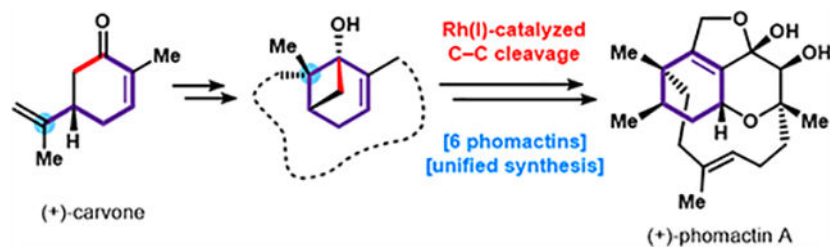
Complete contact information is available at: <https://pubs.acs.org/10.1021/jacs.0c07316>

ASSOCIATED CONTENT

Supporting Information

The Supporting Information is available free of charge at <https://pubs.acs.org/doi/10.1021/jacs.0c07316>.

Experimental details and spectroscopic data, including Supporting Figures 1–5 and Supporting Tables 1–14 (PDF)



## INTRODUCTION

Terpenoids have long held the fascination of the chemical community, in no small part due to their varied and intriguing molecular architectures and the challenge they pose to de novo chemical synthesis.<sup>1</sup> Terpenoid natural products primarily consist of a hydrocarbon skeleton, punctuated by varying degrees of oxidation/oxygenation. Because of their inherent carbocyclic nature, the synthesis of terpenoids has been dominated by methods for the precise construction of carbon–carbon (C–C) bonds. In this context, C–C bond construction can begin either from acyclic isoprene-derived units which proceed through bioinspired polyene cyclizations,<sup>2</sup> or in a stepwise manner by substitution around the periphery of a readily available carbocyclic starting material to introduce target-relevant structural complexity (Figure 1A). The latter strategy can be effective, particularly when readily available carbocycles with the requisite functional handles are embedded within a larger natural product framework.<sup>3</sup> However, a large number of terpenoid natural products contain densely functionalized carbocycles that do not directly correspond to an easily accessible precursor carbocycle.

Many significant advancements in terpenoid total synthesis can be traced to the rearrangement of abundant carbocyclic feedstocks. The skeletal or peripheral remodeling of “chiral pool” compounds (e.g., Figure 1B) involving C–C bond formation and cleavage is a particularly valuable approach to access new enantioenriched scaffolds that might otherwise be difficult to build from classical C–C bond-forming processes that functionalize only the periphery of a ring (as in Figure 1A).<sup>4</sup> The possibility of C–C bond formation/cleavage sequences often enables non-intuitive retrosynthetic disconnections that can greatly simplify a synthesis if used strategically. While various pericyclic and carbocation-based rearrangements have been successfully enlisted in this regard, the toolbox of rearrangement reactions for carbocyclic skeletons remains relatively limited and is often driven by the stereoelectronic effects inherent to the substrate carbocycle.<sup>5</sup> In contrast, transition-metal-mediated C–C bond cleavage processes provide promising new avenues for remodeling carbon scaffolds that often proceed with selectivities orthogonal to “classical” rearrangements (i.e., those catalyzed by Brønsted or Lewis acids, or thermally driven).<sup>6</sup> When combined with or initiated by a bond-forming process, transition-metal-mediated C–C bond cleavage has the potential to access novel carbocyclic scaffolds and provide non-intuitive approaches to complex molecule synthesis.<sup>7</sup>

In this Article, we report our studies on the underutilized potential of metal-mediated C–C bond cleavage processes of hydroxylated pinene derivatives derived from (+)-carvone to

form uniquely substituted cyclohexenones. This skeletal remodeling process has been applied in the asymmetric and unified total synthesis of the phomactin terpenoids.

### Structural Features of the Phomactins.

The phomactin natural products are a small class of terpenoids exemplified by phomactin A (**1**), the first of the secondary metabolites to be discovered in this class (Figure 2A).<sup>8</sup> Phomactin A was first isolated from a *Phoma* species of marine fungus in 1991 during a search for fungal metabolites that display platelet-activating-factor receptor (PAFR) antagonism.<sup>9</sup> Further investigation into this *Phoma* species resulted in the isolation of additional phomactin natural products including phomactin B2 (**2**), phomactin G (**3**), and several other congeners.<sup>10</sup> More recently in 2018, Berlinck and co-workers disclosed six new phomactin terpenoids, including phomactin R (**4**) and phomactin T (**5**), which were isolated from the fungus *Biatriospora* sp. CBMAI 1333.<sup>11</sup> To date, there have been 27 distinct phomactin natural products isolated and disclosed by various groups.<sup>12</sup>

The phomactin terpenoids are characterized by an unusual bicyclo[9.3.1]pentadecane core that comprises their carbocyclic framework (highlighted in green for phomactin P (**6**), Figure 2A). As a result, each natural product contains a densely functionalized cyclohexyl ring, bridged by a macrocyclic “strap”. Phomactin A (**1**), the flagship molecule in this terpenoid class, is arguably the most structurally complex congener. It contains an oxadecalin framework embedded in its core structure as well as a highly sensitive hydroxylated dihydrofuran structural motif, which is also present in phomactin G (**3**) and Sch 49027 (**7**).

### Previous Synthetic Studies.

The phomactin natural products have garnered much attention from the synthetic community over the past 30 years.<sup>8</sup> In addition to the total syntheses of several members (**1**, **2**, **3**, and **8**) that had been completed prior to our studies, there exist over 25 “progress toward” studies, featuring diverse strategies for the construction of either the common bicyclo[9.3.1]pentadecane core or the reduced furanochroman functional group that is unique to phomactin A (**1**).<sup>13</sup> The sheer number of studies toward the syntheses of these natural products highlights the synthetic challenge associated with preparing these molecules. In particular, formation of the densely functionalized cyclohexyl core in enantioenriched form has proven surprisingly difficult.

The first completed total synthesis of a phomactin congener was that of (+)-phomactin D (**8**), which was reported by Yamada and co-workers in 1996 (Figure 2B).<sup>14</sup> This synthesis of the enantioenriched natural product set an important precedent for future approaches by independently constructing the functionalized cyclohexyl system (**13**) and the linear “strap” portion (**14**) and then effecting a convergent coupling to forge the macrocycle at a late stage. As is described within, our own strategy for a unified synthesis of the phomactins benefitted immensely from many principles first highlighted by Yamada. However, the Yamada synthesis also revealed the difficulty in building the cyclohexane fragment (see **13**, highlighted in blue), requiring 25 steps and many functional group interconversions to prepare this complex piece.

In 2002, Pattenden and co-workers were the first to complete a total synthesis of ( $\pm$ )-phomactin A (Figure 2C).<sup>15</sup> Although this was a racemic synthesis, the unique strategy employed by Pattenden et al. to introduce the “strap” motif (**16**) early in the route led to a relatively short total synthesis (19 steps longest linear sequence). Furthermore, deoxygenation of an intermediate compound prior to reaching **17** in the Pattenden route led to the racemic synthesis of ( $\pm$ )-phomactin G (**3**).<sup>16</sup> Shortly thereafter, in 2003, the first asymmetric synthesis of (+)-phomactin A (**1**) was reported by Halcomb and co-workers (Figure 2D).<sup>17</sup> The Halcomb synthesis utilized a convergent strategy that brought together the cyclohexyl core **20** and the linear “strap” **21**, which had been prepared separately. However, a sequential bond formation strategy was employed, and elaboration of the initial “chiral pool” compound (+)-pulegone (**18**) to cyclohexene **20** was remarkably challenging, requiring 18 steps.

In the intervening years before our own studies of the phomactins, an inventive 22-step synthesis of ( $\pm$ )-phomactin B2 (**2**) was accomplished by Wulff and co-workers,<sup>18</sup> as well as a 37-step synthesis of ( $\pm$ )-phomactin A (**1**) by Hsung and co-workers that was highly illuminating in pointing out many of the hidden challenges in approaching the syntheses of these molecules.<sup>19</sup> Recently, a formal synthesis of (+)-phomactin A (**1**) was disclosed by Lee and co-workers that intercepts a late-stage intermediate in the Halcomb route.<sup>20</sup> While there have been many creative strategies developed to synthesize phomactin-type terpenoids, we recognized that there still existed an unmet synthetic challenge, namely, an efficient strategy that could provide a unified route to numerous phomactin congeners in enantioenriched form. Our solution to this problem was published in 2018, enabling the asymmetric total synthesis of six phomactin congeners from a common late-stage synthetic intermediate and showcasing the power of a C–C bond formation/cleavage strategy in terpenoid synthesis.<sup>11</sup> Here, we provide both a full account of the evolution of our synthetic strategy and a demonstration of the intricacies of metal-mediated C–C bond cleavage on complex substrates, discovered over the course of our total synthesis endeavor.

## RESULTS AND DISCUSSION

### Retrosynthetic Considerations.

Our synthetic strategy was built on the recognition that the central cyclohexyl ring of the phomactins could be accessed efficiently from the abundant “chiral pool” compound (+)-carvone (**22**, Figure 3A). While the intact carvone skeleton does not map directly onto the phomactin terpenoid framework, we pictured a “rearranged” skeleton such as **24** as an ideal synthetic partner. In order to achieve the requisite carvone rearrangement, we sought to build on earlier methodology studies from our research group on C–C bond cleavage/functionalizations. Specifically, (+)-carvone can be converted into the dihydroxylated pinene derivative **23** using a previously reported two-step procedure involving epoxidation of **22** with *m*-chloroperoxybenzoic acid (mCPBA), followed by reductive coupling of the epoxide and carbonyl moieties with in situ generated Cp<sub>2</sub>TiCl.<sup>21</sup> Subjecting cyclobutanol **23** to substoichiometric amounts of [Rh(cod)OH]<sub>2</sub> results in scission of the C4–C5 bond of the cyclobutanol, thus effecting the skeletal rearrangement of carvone into cyclohexenone **24**.<sup>22</sup>

Cleavage of the cyclobutanol occurs selectively, resulting in the cleavage of the stronger C4–C5 bond over the weaker C2–C5 bond.<sup>23</sup>

Cyclohexenone **24** readily maps onto the congested cyclohexene core structure of the phomactin natural products, leading to the enantiospecific formation of this stereochemically demanding portion of the phomactins in just three steps from carvone. Furthermore, elaboration of cyclohexenone **24** into a late-stage common synthetic intermediate (**25**) could be accomplished by the addition of a simple linear polyene such as **26** (Figure 3B), similar to the pioneering work showcased by Yamada and co-workers.<sup>14</sup> This common synthetic intermediate bears functionality common to all the phomactin congeners and contains key orthogonal functional handles for further late-stage diversification into a wide variety of natural products.

Key to the success of our carvone skeletal remodeling strategy would be tactical manipulations of not just the functional groups of cyclohexenone **24** but also those of intermediate cyclobutanol **23**. In fact, we first envisioned several potential benefits of delaying C–C bond cleavage until after macrocyclization (Figure 3C). Here, the common synthetic intermediate (**25**) could arise from enone **27** via methylenation and selective oxidation at the bis-allylic C2 position. Enone **27** in turn could arise from cyclobutanol **28**, first through intramolecular sulfone alkylation to close the macrocycle (in line with the precedent of refs 13l and 14), followed by selective cleavage of the cyclobutanol to establish the *syn*-disposed vicinal methyl groups of enone **27**. We hypothesized that, by delaying the cyclobutanol opening, the potentially challenging macrocyclization step<sup>24</sup> would be facilitated by the rigid scaffold of the bicyclo[3.1.1] system.<sup>25</sup> Indeed, examination of 3D models indicated that cyclobutanol **28** was locked in a productive conformation for cyclization, placing the methylene sulfone moiety in an axial position (see Figure 3C). Additionally, delaying cyclobutanol fragmentation would provide a rigid template to exploit in a hydroxy-group-directed C–H functionalization of the allylic methyl group of cyclobutanol **23**.

### Initial Strategy: $\pi$ -Allyl Stille Fragment Coupling.

Initial studies were undertaken to exploit the tertiary hydroxy group in cyclobutanol **23** as a directing group for C(sp<sup>3</sup>)–H functionalization. After *tert*-butyldimethylsilyl (TBS) protection of the primary hydroxy group of **23**, the one-pot procedure developed by Hartwig and co-workers for silylation of alcohol groups followed by dehydrogenative C–H silylation gave oxasilolane **29** in 80% yield (Scheme 1).<sup>26</sup> Importantly, this reaction is completely chemoselective toward functionalization at the allylic methyl position over the alkyl methyl group. This selectivity arises from both the slight activating ability of the neighboring  $\pi$ -system and a favorable dihedral angle between the allylic methyl group and the silyloxy group, which is close to 0°. In our envisioned ideal scenario, the allyl silane functionality of **29** would be utilized in a Hiyama-type coupling to achieve direct vinylation at C2. However, with isobutenyl bromide as a model cross-coupling partner, the desired skipped diene **30** was not observed. Instead, cyclohexenone **31** was formed as the sole product, presumably through an Uemura-type C–C cleavage/cross-coupling sequence.<sup>27</sup> Unfortunately, any type of direct coupling at C2 from oxasilolane **29** or its derivatives was unsuccessful, prompting

us to investigate a polarity-reversal strategy. In preparation for these studies, Tamao–Fleming oxidation of oxasilolane **29** yielded the corresponding free diol, which was selectively acetylated to give allylic acetate **32**. Allylic acetate **32** proved competent as a coupling partner with a range of vinyl nucleophiles.<sup>28</sup>

For the purposes of the total synthesis, prior to exploring vinyl cross-couplings of allylic acetates related to **32** en route to the phomactins, primary alcohol **23** was converted to phenyl sulfide **33** (Scheme 2) to provide a future handle for macrocyclization and avoid the use of the TBS protecting group that would be required otherwise. Iridium-catalyzed dehydrogenative silylation was effected on **33** to functionalize the allylic position; however, a subsequent Tamao–Fleming oxidation proved challenging and led to non-specific decomposition. Fortunately, selenium dioxide proved capable of directly effecting allylic oxidation of **33** to provide allylic acetate **34** after mono-acetylation. Oxidation of phenyl sulfide **34** to sulfone **35** with ammonium heptamolybdate and hydrogen peroxide proceeded smoothly. Interestingly, this sulfide-to-sulfone conversion was found to be uniquely successful on this particular substrate. Attempted sulfide oxidation on compound **33** resulted in substantial rearrangement to [2.2.1]bicycle **36**, caused by the nucleophilic alkene engaging the oxidant. It appears that, in **34**, the acetate group effectively suppressed this unwanted reactivity because of its electron-withdrawing nature, leading to clean oxidation to sulfone **35**.

Allylic acetate **35** served as an excellent substrate for a  $\pi$ -allyl Stille reaction<sup>29</sup> with vinyl stannane **38**<sup>30</sup> to form the coupled product **39** in 55% yield along with 25% of the Grob fragmentation product **40**. This fragmentation could be partially suppressed by converting the tertiary hydroxy group of **35** to a trimethylsilyl (TMS) ether, thus forming the desired adduct **41** in 61% yield. To complete the macrocycle, primary alcohol **41** was converted to allylic bromide **42**, which upon treatment with sodium bis(trimethylsilyl)amide (NaHMDS) cleanly afforded the macrocyclic product **43** with no trace of competing Grob fragmentation.<sup>31</sup> The TMS group was readily cleaved under the action of an acidic Amberlyst resin and methanol to give **44**.

### Divergent Reactivity in the Rh(I)-Catalyzed C–C Bond Cleavage.

Our access to **44** demonstrated that the rigid [3.1.1]bicycle could be employed in the rapid construction of the carbocyclic framework of the phomactin natural products. With the macrocycle in place, we next investigated the selective scission of the embedded cyclobutanol. It is known that Rh(I) catalysts are efficient at effecting the desired C–C cleavage/protodemetalation on simpler substrates.<sup>32</sup> However, the cyclobutanol ring opening of a complex substrate such as **44** was unprecedented. We were uncertain as to (A) how the additional strain resident in the macrocycle would affect the selectivity of the C–C bond cleavage, (B) whether Grob fragmentation would predominate, or (C) whether the presence of several double bonds in the substrate might bind the Rh complex in an unproductive manner or participate in unwanted side reactions.

We were pleased to find that heating cyclobutanol **44** with 10 mol% [Rh(cod)OH]<sub>2</sub> to 40 °C in deuterated benzene resulted in the desired C–C bond cleavage. However, it did not result



in formation of desired cyclohexenone **45**, but instead yielded the related  $\beta,\gamma$ -unsaturated ketone **46** (Scheme 3A).  $\beta,\gamma$ -Unsaturated ketone **46** presumably forms via the intermediacy of alkyl rhodium species **47**, which undergoes a 1,3-Rh shift to give the allylic rhodium species **48**.<sup>22</sup> Protodemetalation with protonation occurring at the  $\alpha$  position then furnishes the observed product. To probe this mechanistic hypothesis, small amounts of D<sub>2</sub>O were added to the reaction mixture. A deuterium incorporation of 90% was observed at the position  $\alpha$  to the carbonyl (see *d*-**46**), whereas no deuterium incorporation was observed on the methyl group (i.e., at C19), supporting an intramolecular rhodium shift that results in protonation at C19.

Interestingly, unconjugated enone **46** could not be readily purified and isolated. Upon its exposure to air, rapid oxidation occurred to give a 1:1 mixture of hydroxy enone **49** and enedione **50** in a combined yield of 50% (Scheme 3B).<sup>33</sup> Although unexpected, we recognized that this facile oxidation could be beneficial since several of the phomactin natural products bear oxygenation at C13 (e.g., phomactins B2 (**2**) and K (**9**), see Figure 2). One possible explanation for this facile oxygenation is that the weakened  $\alpha$  C–H bond of **46** allows for facile hydrogen atom abstraction to give allylic radical **51**.<sup>34</sup> Radical combination with triplet oxygen would form allylic peroxy species **52**. This peroxy intermediate could either undergo in situ reduction to yield hydroxy enone **49** or suffer the formal loss of a hydroxyl radical to give enedione **50**. Importantly, hydroxy enone **49** was found to be stable and did not oxidize to enedione **50** over prolonged exposure to air. Furthermore, hydroxy enone **49** could be selectively formed if dimethyl sulfide was added to the reaction mixture immediately upon exposure of unconjugated enone **46** to air (Scheme 3C), supporting the hypothesis that both oxidation products arise from peroxy species **52**.

Optimization of the Rh(I)-catalyzed C–C cleavage for conjugated enone **45** required a subsequent olefin isomerization. Although employing various bases was unsuccessful, switching the solvent from benzene to methanol enabled clean conversion to desired enone **45** in 89% yield (Scheme 3C). This ring cleavage/olefin isomerization transformation seems to occur through a pathway analogous to that shown in Scheme 3A by first forming  $\beta,\gamma$ -enone **46**, followed by olefin isomerization. Conducting the reaction in deuterated methanol clearly shows the rapid formation of  $\alpha$ -deuterio ketone *d*-**46**, which slowly converts to  $\gamma$ -deuterio enone *d*-**45**, consistent with this proposed mechanism.<sup>35</sup>

At this point, we were emboldened by the fact that the Rh(I)-catalyzed C–C bond cleavage was achievable on this late-stage, complex substrate (i.e., **44**). Additionally, by subtly altering the conditions for this C–C cleavage transformation, cyclobutanol **44** could be converted into either cyclohexenone **45** or its hydroxylated variant, **49**. However, to fully elaborate either of these compounds into phomactin natural products, selective oxygenation at the doubly allylic position (C2) was required. Unfortunately, oxygenation at C2 proved to be an extremely challenging task. Due to the constrained macrocycle, the two  $\pi$  systems flanking C2 are not coplanar, resulting in less activation than would be anticipated for a doubly allylic position. Furthermore, upon the generation of a radical at C2, rapid olefin isomerization occurred to form an undesired 1,3-diene system.<sup>36</sup> Given these challenges,



which were not resolved even after exhaustive experimentation, we settled on examining synthetic routes where oxygenation at C2 was preinstalled.

### Revised Strategy: Fragment Coupling Using a 1,2-Addition into an Aldehyde.

We recognized that instead of appending the linear “strap” portion to allylic acetate **37**, a coupling partner with a higher oxidation state at C2 would maintain oxygenation after the coupling reaction. To this end, 1,2-addition to aldehyde **53**, accessed in three steps from cyclobutanol **33**, was pursued (Scheme 4).<sup>37</sup> Treatment of vinyl iodide **54**<sup>38</sup> with *tert*-butyl lithium at low temperatures followed by the addition of aldehyde **53** readily gave bis-allylic alcohol **55** in 68% yield as a 5:1 mixture of diastereomers. By advancing the major diastereomer, formation of the macrocycle occurred in a similar fashion as described for the previous route (see Scheme 2). The newly formed hydroxy group at C2 in **55** was first protected as the TBS ether, and then sulfide oxidation was performed to give sulfone **56**. Oxidative cleavage of the *p*-methoxybenzyl (PMB) group followed by bromination yielded allylic bromide **57**, which upon treatment with NaHMDS cleanly afforded the macrocycle **58** in 91% yield. Buffered conditions (tris(dimethylamino)sulfonium difluoro-trimethylsilicate (TASF) and acetic acid) were employed for silyl group removal because the previously employed acidic conditions resulted in ionization of the bis-allylic TBS ether group, whereas base-promoted cleavage conditions resulted in Grob fragmentation of **58**. Depending on the reaction temperature, cleavage of primarily one or both silyl ethers could be achieved to give cyclobutanol **59** or diol **60**, respectively.

Regarding the Rh(I)-catalyzed C–C bond cleavage step for cyclobutanol **59**, the presence of a silyloxy group at C2 brought about a different reactivity profile as compared to the previously employed cyclobutanol **44**. Subjecting silyloxy cyclobutanol **59** to 10 mol% [Rh(cod)OH]<sub>2</sub> in benzene resulted in the formation of triene **61**, presumably arising from  $\beta$ -silyloxy elimination of an intermediate allyl rhodium species (**62**, Scheme 5). As in our previous studies on cyclobutanol openings, switching the solvent from benzene to methanol resulted in the formation of the desired cyclohexenone **63**. Interestingly, and in direct contrast to the conversion of **44** to **45**, when the reaction was conducted in deuterated methanol, deuterium incorporation was observed at C19 (the newly unveiled methyl group) and not at the  $\gamma$  position of enone **63**.<sup>39</sup> This observation strongly supports protodemetalation at C19 outcompeting the 1,3-Rh shift on alkyl rhodium species **64** in the presence of methanol. This outcome could be due to the additional steric bulk of the TBS ether suppressing the 1,3-Rh shift and reducing the formation of the competing  $\beta$ -silyloxy elimination product. Of note, diol **60** also participated in the Rh(I)-catalyzed C–C bond cleavage process, producing the desired cyclohexanone **65** in 49% yield.

Next, we investigated the reductive removal of the sulfone moiety in macrocycle **65**, fully aware that doing so in the presence of an enone moiety could be problematic due to its susceptibility to reduction (Scheme 6). Indeed, several conditions (such as samarium iodide) only served to reduce the enone, whereas milder reductants did not provide any reactivity. Interestingly, Birch-type dissolving metal conditions yielded fully reduced diol **66** as the minor product and cyclopropanol **67** as the major product. Presumably, cyclopropanol **67** formed from the addition of an incipient carbanion into the carbonyl group.<sup>40</sup> While

cyclopropanol **67** was somewhat unstable, it was amenable to selective C–C cleavage by heating the mixture with sodium methoxide to give enone **68**.<sup>41</sup> In a way, the fortuitously formed cyclopropanol likely served as an in situ “protecting group” for the enone moiety, preventing further reduction under the harsh dissolving metal conditions.

At this stage, a single carbon atom remained to be installed through methylenation of enone **68** to complete the phomactin framework. Although seemingly trivial, this one-carbon addition proved to be another major challenge. The majority of carbon-based nucleophiles that we investigated did not react with enone **68** (e.g., phosphonium salts or alkyl zinc reagents<sup>42</sup>), whereas a few added in a 1,4-fashion (e.g., methyl lithium). From an examination of the conformation of **68**, it is clear that the Bürgi–Dunitz approach to the carbonyl group is extremely hindered. The macrocyclic “strap” sits directly underneath the cyclohexenone ring system, completely blocking this face. Moreover, the macrocycle locks the cyclohexenone into a conformation that places the C19 methyl group in a pseudo-axial position, severely obstructing a Bürgi–Dunitz approach to the carbonyl group from the top face.<sup>19</sup> Given the challenges associated with a direct 1,2-addition to encumbered enone **68**, we took a few steps back to again revise our synthetic strategy and incorporate the C20 group earlier in the sequence.

### Successful Strategy to the Phomactins: Early-Stage Cyclobutanol Fragmentation.

In order to efficiently install the carbon unit at C20, we recognized that cyclobutanol fragmentation and subsequent methylenation would be required prior to macrocyclization (Scheme 7). In our revised and ultimately successful synthetic approach, unified access to the phomactin terpenoids would be accomplished through selective oxygenation of common synthetic intermediate **25**, which could be formed through macrocyclization of sulfone **69**. As shown previously, addition of the “strap” portion (**70**) can be accomplished by 1,2-addition into aldehyde **71**. We posited that carbonyl methylenation would be viable on a less encumbered substrate such as enone **72**, which in turn can arise from C–C bond cleavage of cyclobutanol **33**.

The synthesis sequence commenced with cyclobutanol **33**, which upon exposure to 7.5 mol % of [Rh(cod)OH]<sub>2</sub> resulted in the desired C–C bond fragmentation (Scheme 8). Again, the use of methanol as solvent was required to achieve optimal yields. Sulfide-to-sulfone oxidation provided enone **72**. Although direct methylenation of enone **72** was still troublesome, we were pleased to find that, unlike the more sterically congested **68**, treatment with methyl lithium added a methyl group in a 1,2-fashion to enone **72**. Subjecting the resulting 1,2-adduct to the Burgess reagent provided a two-step methylenation. Allylic oxidation at that stage with excess selenium dioxide provided aldehyde **71**.

Following a similar aldehyde 1,2-addition protocol as before (i.e., **53** → **55**), vinyl iodide **70**<sup>43</sup> was treated with *tert*-butyl lithium and added to aldehyde **71** at low temperatures to afford bis-allylic alcohol **73** as a 1:1 mixture of diastereomers. Protection of the resulting hydroxy group with a 2-(trimethylsilyl)ethoxymethyl (SEM) group followed by cleavage of the TBS group and bromination of the primary alcohol group yielded allylic bromide **74**. Macrocyclization proceeded smoothly to give macrocycle **75**, even without the

conformational bias imparted by the rigid [3.1.1]bicyclic scaffold that had been previously employed (i.e., **42** → **43** and **57** → **58**). At this stage, reductive desulfonation under Birch conditions afforded a modest amount of desired product **76**. However, by switching to sodium–mercury amalgam, **76** was formed in a satisfactory 75% yield. Finally, cleavage of the SEM group with tetra-*n*-butylammonium fluoride (TBAF) in *N,N'*-dimethylpropyleneurea (DMPU) gave alcohol **25** as a 1:1 mixture of diastereomers.<sup>44</sup> Although the stereochemistry at C2 is ultimately inconsequential, we found that only one of the two alcohol diastereomers was competent in subsequent chemistry. Therefore, a one-pot oxidation/reduction sequence was employed to give **25** as a single diastereomer. In this way, the desired common intermediate to the phomactins (**25**) is accessible in 16 steps from (+)-carvone, achieved through the strategic application of C–C bond cleavage of carvone-derived cyclobutanol **33**. This system is readied for diversification into numerous phomactin congeners.

### Synthesis of Phomactins R, P, and K.

With the ultimate goal of synthesizing structurally complex phomactins such as phomactins A and T, we initially set our sights on advancing common intermediate **25** to the relatively less functionalized phomactin R (**4**, Scheme 9). Initial directed epoxidation studies with VO(acac)<sub>2</sub> and *tert*-butyl hydroperoxide (TBHP) resulted in a complex mixture of epoxides arising from constitutional isomers as well as diastereomers. At low temperatures, switching the catalyst from VO(acac)<sub>2</sub> to VO(OEt)<sub>3</sub> resulted in improved selectivity, forming the desired epoxide (**77**) in 72% yield.<sup>45</sup> Nuclear Overhauser effect (NOE) correlations between the epoxide  $\alpha$ -proton and the allylic methyl group aided in confirming the relative configuration of epoxide **77**. Further confirmation was achieved upon alcohol oxidation with Dess–Martin periodinane (DMP) to yield phomactin R (**4**), which provided data fully consistent with those reported in the literature, completing the total synthesis in 18 steps from (+)-carvone.

In line with the presumed biosynthetic pathway<sup>46</sup> to these natural products, sequential oxygenation of phomactin R (**4**) should lead to the formation of phomactins P (**6**) and K (**9**), respectively. Indeed, epoxidation of phomactin R (**4**) with dimethyldioxirane (DMDO) furnished phomactin P (**6**); however, the major product was the diastereomeric compound resulting from epoxidation of the other alkene face. Switching the oxidant from DMDO to mCPBA reversed the diastereoselectivity and produced phomactin P (**6**) in 66% yield. Phomactin P (**6**) was further oxidized at C13 under Doyle oxidation conditions<sup>47</sup> using TBHP in the presence of Rh<sub>2</sub>(cap)<sub>4</sub> to furnish phomactin K (**9**) following 1,8-diazabicyclo[5.4.0]undec-7-ene (DBU)-promoted loss of *tert*-butanol.

### Structural Revision of Sch 49027 and Synthesis of Phomactins A and T.

During the course of our epoxidation studies on common intermediate **25**, we discovered that a second epoxidation can occur to give bis-epoxide **78** if the reaction is allowed to warm to 0 °C (Scheme 10). Again, the use of VO(OEt)<sub>3</sub> was critical for the successful formation of the bis-epoxide. We recognized that further oxidation to bis-epoxyketone **79** afforded a compound at the appropriate oxidation state to form phomactin A (**1**) following an epoxide-opening cascade. In theory, a water molecule could serve to open both epoxides and form

tetrahydropyranone derivative **80**. Furthermore, water-mediated allylic transposition could give phomactin A (**1**) following hemiketalization. Unfortunately, this cascade cyclization reaction was not realized in our hands. In fact, no reactivity was observed upon heating bis-epoxyketone **79** with water, and the addition of Lewis acids either failed to facilitate reactivity or led to a complex mixture of non-specific decomposition products.

A more controlled and stepwise epoxide opening was next explored from bis-epoxy alcohol **78**. After considerable experimentation, we found that utilizing  $\text{Me}_4\text{NBH}(\text{OAc})_3$  as a Lewis acid resulted in a mixture of compounds (**81**, **82**, and **83**), all seemingly arising from the same allylic cation (**81** from a Meinwald rearrangement; **82** and **83** from acetate trapping).<sup>48</sup> The addition of  $\text{CsOAc}$  to the reaction mixture resulted in a slight increase in the relative amount of acetate **83** that was formed, whereas adding 18-crown-6 to this mixture resulted in complete selectivity for this C20 acetate (**83**). The free diol (**84**) was liberated from **83** by filtration over a pad of silica gel.

Selective mono-oxidation of diol **84** with DMP was accomplished at 0 °C to yield ketone **85**. Surprisingly, quenching the reaction mixture with NaOMe (intended to cleave the acetyl group) resulted in a compound that matched the spectral data for Sch 49027. Although double bond isomerization could not be ruled out, the more likely product of the reaction is allylic alcohol **86**, which led us to speculate that **86** is the true structure of Sch 49027 and not the originally proposed enol-containing **7**. The revised structure for Sch 49027 (**86**) was corroborated by careful analysis of several 2D NMR experiments—key HMBC correlations are indicated in Scheme 10, and COSY correlations were observed between all the protons in the cyclohexyl ring system.<sup>49</sup>

Epimerization of the secondary allylic hydroxy group of Sch 49027 (**86**) was expected to lead to spontaneous cyclization (see allylic alcohol **88**) and formation of phomactin A (**1**). In practice, oxidation of diol **84** with DMP at room temperature led to the formation of ketone **87** after quenching with NaOMe to cleave the acetyl group and achieve spontaneous hemiketalization. Treatment of ketone **87** with  $\text{NaBH}_4/\text{CeCl}_3$  or  $\text{LiAlH}_4$  did not lead to formation of phomactin A (**1**) but instead led to the exclusive formation of Sch 49027 (**86**). This alternative synthesis of **86** further corroborates the revised structure of this natural product. Switching to a sterically larger reductant such as DIBAL-H resulted in a 1:2 mixture of phomactin A (**1**) and Sch 49027 (**86**), and utilizing Red-Al gave a 2.2:1 mixture of the natural products, ultimately yielding phomactin A (**1**) in 51% and completing its total synthesis in 20 steps from (+)-carvone.

The synthesis of the structurally unique phomactin T (**5**) required additional oxidation at C20. To achieve this, allylic epoxide **78** was subjected to  $\text{Me}_4\text{NBH}(\text{OAc})_3$  as before and then quenched with NaOMe to give triol **89** (Scheme 11). Global oxidation of triol **89** with DMP at 60 °C successfully delivered aldehyde **90**.<sup>50</sup> Pinnick oxidation of aldehyde **90** was unsuccessful. However, we were excited to find that oxidation of **90** with mCPBA in wet dichloromethane (DCM) directly furnished lactol **92**. This process likely occurs first through diastereoselective epoxidation to give epoxy-aldehyde **91**, then aldehyde hydration followed by a transannular epoxide opening. Lactol **92** proved unstable to isolation, so a one-step protocol was developed wherein manganese dioxide was added along with mCPBA to

directly furnish phomactin T (**5**) from aldehyde **90**, completing the total synthesis of this topologically unique congener in 20 steps from (+)-carvone.

## CONCLUSION

The phomactin terpenoids continue to provide fertile ground for pushing the limits of modern synthetic chemistry. By leveraging a Rh(I)-catalyzed C–C bond cleavage reaction, we were able to access “rearranged” carvone skeletons and address a key challenge in phomactin synthesis—the enantiospecific construction of the congested cyclohexyl core. This key recognition of the relationship between carvone and the cyclohexyl core of the phomactins enabled the development of efficient syntheses of diverse phomactin congeners in enantioenriched form, culminating in the syntheses of phomactins A, K, P, R, and T and Sch 49027, with the latter structure reassigned as a result of this total synthesis effort. Each of these terpenoids was synthesized in 18–20 steps from (+)-carvone. Additionally, each natural product was produced in just 2–4 steps from a common late-stage intermediate (**25**) through a series of carefully choreographed oxidation or rearrangement steps, underscoring the unified approach that was developed.

As a result of this total synthesis endeavor, many intricacies of transition-metal-mediated C–C bond cleavage have become apparent. Rh(I)-catalyzed fragmentation of cyclobutanols **44** and **59** revealed alternative processes that can occur on complex substrates, for example, rhodium shift, deconjugation, oxygenation, or silyloxy elimination. Additionally, slight differences in substrates or reaction conditions were found to influence the protodemetalation step, a phenomenon uniquely brought to light through the application of C–C cleavage in a complex molecule setting.

More fundamentally, this work has demonstrated the power of strategic C–C bond cleavage reactions in total synthesis. While our strategy of cyclobutanol formation followed by C–C cleavage might be non-intuitive, the overall goal of remodeling carbocyclic skeletons warrants further investigation and applications by the chemical community. Furthermore, transition-metal-mediated C–C cleavage processes that concurrently forge one or more new bonds (via cyclization or coupling) uniquely hold the power to deconstruct and reconstruct carbocyclic frameworks in rapid fashion. Future advancements in simultaneous C–C cleavage and reforming processes, as well as methodologies to selectively cleave C–C bonds in unstrained rings, will further advance the field of complex natural product synthesis.<sup>51</sup>

## Supplementary Material

Refer to Web version on PubMed Central for supplementary material.

## ACKNOWLEDGMENTS

R.S. thanks the National Institutes of General Medical Sciences for support (R35 GM130345). P.R.L. thanks the National Science Foundation for a graduate fellowship. Y.K. thanks the Japan Society for the Promotion of Science (JSPS) for an Overseas Research Fellowship, and S.C. thanks the National Science and Engineering Council–Canada (NSERC) for a postdoctoral fellowship. We are grateful to Professor Roberto G. S. Berlinck (University of São Paulo, Brazil) for insightful discussions regarding the phomactins and an enjoyable collaboration on the isolation and biological aspects of our joint research in this area. We thank Dr. Hasan Celik and UC Berkeley’s

NMR facility in the College of Chemistry (CoC-NMR) for spectroscopic assistance. Instruments in CoC-NMR are supported in part by NIH S10OD024998.

## REFERENCES

- (1). Maimone TJ; Baran PS Modern synthetic efforts toward biologically active terpenes. *Nat. Chem. Biol* 2007, 3, 396–407. [PubMed: 17576427]
- (2). Yoder RA; Johnston JN A Case Study in Biomimetic Total Synthesis: Polyolefin Carbocyclizations to Terpenes and Steroids. *Chem. Rev* 2005, 105, 4730–4756. [PubMed: 16351060]
- (3) (a). Money T; Wong MKC The Use of Cyclic Monoterpenoids as Enantiopure Starting Materials in Natural Product Synthesis. *Stud. Nat. Prod. Chem* 1995, 16, 123–288.(b)Gaich T; Mulzer J Chiral Pool Synthesis: Starting from Terpenes In *Comprehensive Chirality*; Carreira EM, Yamamoto H, Eds.; Elsevier Ltd, 2012; Vol. 2, pp 163–206.
- (4). For rearranged chiral pool compounds, see “level 2” and “level 3” syntheses in the following: Brill ZG; Condakes ML; Ting CP; Maimone TJ Navigating the Chiral Pool in the Total Synthesis of Complex Terpene Natural Products. *Chem. Rev* 2017, 117, 11753–11795. [PubMed: 28293944]
- (5) (a). Ilardi EA; Stivala CE; Zakarian A [3,3]-Sigmatropic rearrangements: recent applications in the total synthesis of natural products. *Chem. Soc. Rev* 2009, 38, 3133–3148. [PubMed: 19847347] (b)*Molecular Rearrangements in Organic Synthesis*; Rojas CM, Ed.; John Wiley & Sons, Inc, 2015.
- (6). For recent reviews in the field of transition-metal-mediated C–C cleavage, see: (a) Marek I; Masarwa A; Delaye P-O; Leibel M Selective Carbon–Carbon Bond Cleavage for the Stereoselective Synthesis of Acyclic Systems. *Angew. Chem., Int. Ed* 2015, 54, 414–429. (b)Souillart L; Cramer N Catalytic C–C Bond Activations via Oxidative Addition to Transition Metals. *Chem. Rev* 2015, 115, 9410–9464. [PubMed: 26044343] (c)Murakami M; Ishida N Potential of Metal-Catalyzed C–C Single Bond Cleavage for Organic Synthesis. *J. Am. Chem. Soc* 2016, 138, 13759–13769. [PubMed: 27726343] (d)Nairoukh Z; Cormier M; Marek I Merging C–H and C–C bond cleavage in organic synthesis. *Nat. Rev. Chem* 2017, 1, 0035. (e)Fumagalli G; Stanton S; Bower JF Recent Methodologies That Exploit C–C Single-Bond Cleavage of Strained Ring Systems by Transition Metal Complexes. *Chem. Rev* 2017, 117, 9404–9432. [PubMed: 28075115]
- (7). For usage of C–C bond cleavage in complex molecule synthesis, see: (a) Hoffmann RW Overbred Intermediates Elements of Synthesis Planning; Springer-Verlag, 2009; pp 106–117.(b)Murakami M; Ishida N Total Syntheses of Natural Products and Biologically Active Compounds by Transition-Metal-Catalyzed C–C Cleavage In *Cleavage of Carbon–Carbon Single Bonds by Transition Metals*; Murakami M, Chatani N, Eds.; Wiley, 2015; Chap. 8, pp 253–272.(c)Wang B; Perea MA; Sarpong R Transition Metal-Mediated C–C Single Bond Cleavage: Making the Cut in Total Synthesis. *Angew. Chem., Int. Ed* 2020, DOI: 10.1002/anie.201915657.
- (8). For a review of the phomactin natural products, see: (a) Goldring WPD; Pattenden G The Phomactins: A Novel Group of Terpenoid Platelet Activating Factor Antagonists Related Biogenetically to the Taxanes. *Acc. Chem. Res* 2006, 39, 354–361. [PubMed: 16700534] (b)Ciesielski J; Frontier A The Phomactin Natural Products from Isolation to Total Synthesis: A Review. *Org. Prep. Proced. Int* 2014, 46, 214–251.
- (9). Sugano M; Sato A; Iijima Y; Oshima T; Furuya K; Kuwano H; Hata T; Hanzawa H Phomactin A; a novel PAF antagonist from a marine fungus *Phoma* sp. *J. Am. Chem. Soc* 1991, 113, 5463–5464.
- (10) (a). Sugano M; Sato A; Iijima Y; Furuya K; Haruyama H; Yoda K; Hata T Phomactins, novel PAF antagonists from marine fungus *Phoma* sp. *J. Org. Chem* 1994, 59, 564–569.(b)Sugano M; Sato A; Iijima Y; Furuya K; Kuwano H; Hata T Phomactin E, F, and G: New Phomactin-group PAF Antagonists from a Marine Fungus *Phoma* sp. *J. Antibiot* 1995, 48, 1188–1190.
- (11). Kuroda Y; Nicacio KJ; Alves da Silva I Jr.; Leger PR; Chang S; Gubiani JR; Deflon VM; Nagashima N; Rode A; Blackford K; Ferreira AG; Sette LD; Williams DE; Andersen RJ; Jancar S; Berlinck RGS; Sarpong R Isolation, synthesis and bioactivity studies of phomactin terpenoids. *Nat. Chem* 2018, 10, 938–945. [PubMed: 30061613]



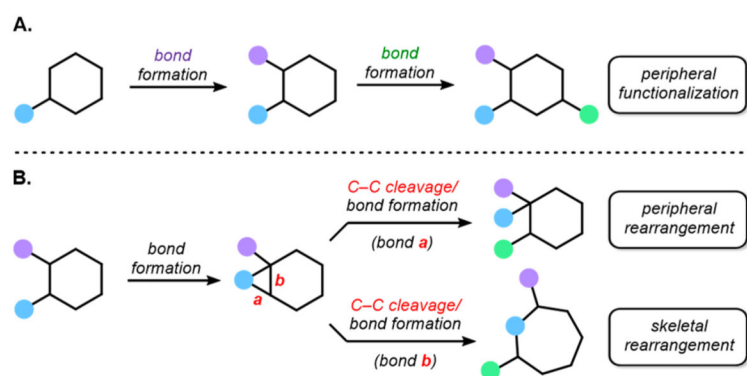
- (12) (a). Chu M; Patel MG; Gullo VP; Truumees I; Puar MS; McPhail AT Sch 47918: a novel PAF antagonist from the fungus *Phoma* sp. *J. Org. Chem* 1992, 57, 5817–5818. (b) Chu M; Truumees I; Gunnarsson I; Bishop WR; Kreutner W; Horan AC; Patel MG; Gullo VP; Puar MSA Novel Class of Platelet Activating Factor Antagonists from *Phoma* sp. *J. Antibiot* 1993, 46, 554–563. (c) Koyama K; Ishino M; Takatori K; Sugita T; Kinoshita K; Takahashi K Phomactin H, a novel diterpene from an unidentified marine-derived fungus. *Tetrahedron Lett.* 2004, 45, 6947–6948. (d) Ishino M; Kiyomichi N; Takatori K; Sugita T; Shiro M; Kinoshita K; Takahashi K; Koyama K Phomactin I, 13-epi-Phomactin I, and Phomactin J, three novel diterpenes from a marine-derived fungus. *Tetrahedron* 2010, 66, 2594–2597. (e) Ishino M; Kinoshita K; Takahashi K; Sugita T; Shiro M; Hasegawa K; Koyama K Phomactins K–M, three novel phomactin-type diterpenes from a marine-derived fungus. *Tetrahedron* 2012, 68, 8572–8576. (f) Ishino M; Kamauchi H; Takatori K; Kinoshita K; Sugita T; Koyama K Three novel phomactin-type diterpenes from a marine-derived fungus. *Tetrahedron Lett.* 2016, 57, 4341–4344.
- (13) (a). Foote KM; Hayes CJ; Pattenden G Synthetic studies towards phomactin A. Concise synthesis of the novel tricyclic furanochroman system. *Tetrahedron Lett.* 1996, 37, 275–278. (b) Seth PP; Totah NI Studies toward the Tricyclic Core of Phomactin A. Synthesis of the Reduced Furanochroman Subunit. *Org. Lett* 2000, 2, 2507–2509. [PubMed: 10956533] (c) Seth PP; Chen D; Wang J; Gao X; Totah NI The Dihydropyrone Diels–Alder Reaction: Development and Application to the Synthesis of Highly Functionalized 1-Oxa-4-decalones. *Tetrahedron* 2000, 56, 10185–10195. (d) Kallan NC; Halcomb RL Synthesis of the Ring System of Phomactin D Using a Suzuki Macrocyclization. *Org. Lett* 2000, 2, 2687–2690. [PubMed: 10990428] (e) Chemler SR; Danishefsky SJ Transannular Macrocyclization via Intramolecular B-Alkyl Suzuki Reaction. *Org. Lett* 2000, 2, 2695–2698. [PubMed: 10990430] (f) Mi B; Maleczka RE A Nozaki–Hiyama–Kishi Ni(II)/Cr(II) Coupling Approach to the Phomactins. *Org. Lett* 2001, 3, 1491–1494. [PubMed: 11388849] (g) Chemler SR; Iserloh U; Danishefsky SJ Enantioselective Synthesis of the Oxadecalin Core of Phomactin A via a Highly Stereoselective Diels–Alder Reaction. *Org. Lett* 2001, 3, 2949–2951. [PubMed: 11554815] (h) Houghton RJ; Choi S; Rawal VH Efficient Assembly of the Phomactin Core via Two Different Macrocyclization Protocols. *Org. Lett* 2001, 3, 3615–3617. [PubMed: 11700095] (i) Foote KM; John M; Pattenden G Synthesis of the Oxygenated Bicyclo[9.3.1]pentadecane Ring System of Phomactin A using Chromium (II)-mediated Macrocyclisation and Ring Closure Metathesis. *Synlett* 2001, 3, 365–368. (j) Mohr PJ; Halcomb RL Convergent Enantioselective Synthesis of the Tricyclic Core of Phomactin A. *Org. Lett* 2002, 4, 2413–2416. [PubMed: 12098260] (k) Foote KM; Hayes CJ; John MP; Pattenden G Synthetic studies towards the phomactins. Concise syntheses of the tricyclic furanochroman and the oxygenated bicyclo[9.3.1]pentadecane ring systems in phomactin A. *Org. Biomol. Chem* 2003, 1, 3917–3948. [PubMed: 14664383] (l) Balnaves AS; McGowan G; Shapland PDP; Thomas EJ Approaches to the total synthesis of phomactins. *Tetrahedron Lett.* 2003, 44, 2713–2716. (m) Cole KP; Hsung RP Intramolecular Formal oxa-[3 + 3] Cycloaddition Approach to the ABD System of Phomactin A. *Org. Lett* 2003, 5, 4843–4846. [PubMed: 14653688] (n) Cole KP; Hsung RP Unique structural topology and reactivities of the ABD tricycle in phomactin A. *Chem. Commun* 2005, 46, 5784–5786. (o) Ryu K; Cho Y-S; Jung S-I; Cho C-G Regioselective Pd-Catalyzed Synthesis and Application of 3-Methyl-5-bromo-2-pyrone toward Keto-phomactin A. *Org. Lett* 2006, 8, 3343–3345. [PubMed: 16836401] (p) Huang J; Wang H; Wu C; Wulff WD Intramolecular Cyclohexadienone Annulations of Fischer Carbene Complexes: Model Studies for the Synthesis of Phomactins. *Org. Lett* 2007, 9, 2799–2802. [PubMed: 17580880] (q) Teng D; Wang B; Augatis AJ; Totah NI Studies toward the synthesis of phomactin A. An approach to the macrocyclic core. *Tetrahedron Lett.* 2007, 48, 4605–4607. [PubMed: 18575571] (r) You L-F; Hsung RP; Bedermann AA; Kurdyumov AV; Tang Y; Buchanan GS; Cole KP An Enantioselective Synthesis of the ABD Tricycle for (–)-Phomactin A Featuring Rawal’s Asymmetric Diels–Alder Cycloaddition. *Adv. Synth. Catal* 2008, 350, 2885–2891. [PubMed: 20351791] (s) Blackburn TJ; Helliwell M; Kilner MJ; Lee ATL; Thomas EJ Further studies of an approach to a total synthesis of phomactins. *Tetrahedron Lett.* 2009, 50, 3550–3554. (t) Shapland PDP; Thomas EJ Synthesis of precursors of phomactins using [2,3]-Wittig rearrangements. *Tetrahedron* 2009, 65, 4201–4211. (u) Schwartz KD; White JD Synthesis of the Cyclohexane Core of Phomactins and a New Route to the Bicyclo[9.3.1]pentadecane Diterpenoid Skeleton. *Org. Lett* 2011, 13, 248–251. [PubMed: 21162546] (v) Huang S; Du G; Lee C-S Construction of the Tricyclic Furanochroman Skeleton of Phomactin A via the Prins/Conia–Ene Cascade Cyclization



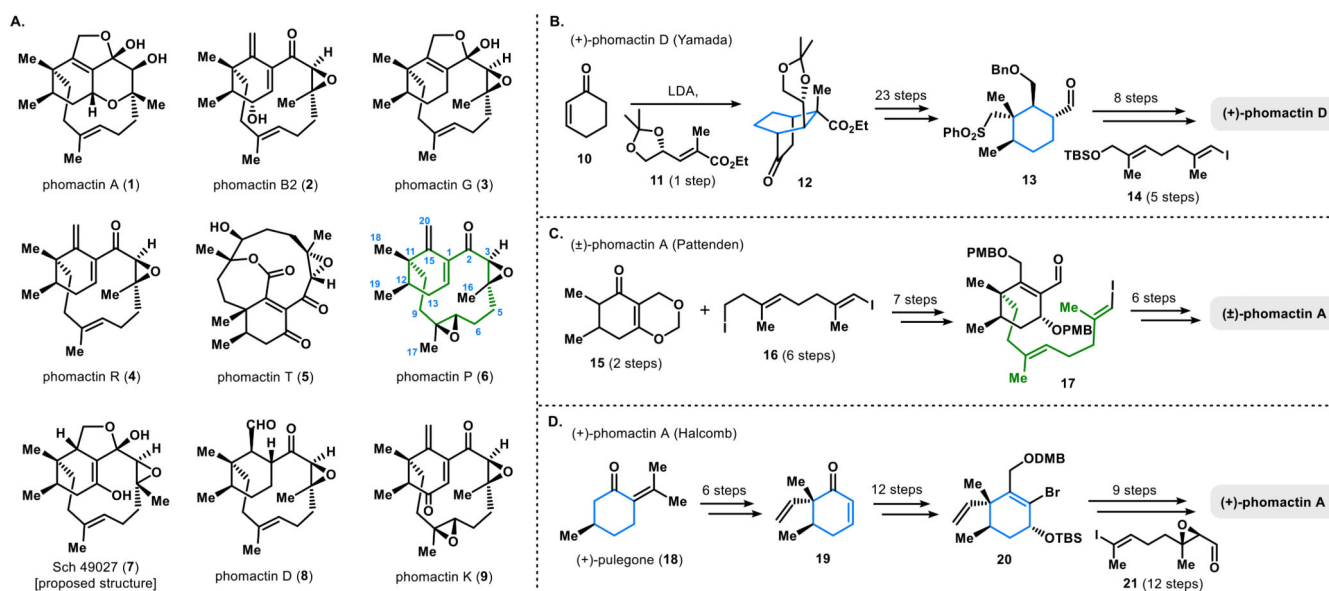
- Approach. *J. Org. Chem* 2011, 76, 6534–6541. [PubMed: 21739982] (w)Ciesielski J; Cariou K; Frontier AJ A Macrocyclic  $\beta$ -Iodoallenolate Intermediate Is Key: Synthesis of the ABD Core of Phomactin A. *Org. Lett* 2012, 14, 4082–4085. [PubMed: 22853449] (x)Ciesielski J; Gandon V; Frontier AJ Cascade Cyclizations of Acyclic and Macrocyclic Alkynes: Studies toward the Synthesis of Phomactin A. *J. Org. Chem* 2013, 78, 9541–9552. [PubMed: 23724905] (y)Burnell ES; Irshad A-R; Raftery J; Thomas EJ Approaches to phomactin A: unexpected late-stage observations. *Tetrahedron Lett.* 2015, 56, 3255–3258. (z)Blackburn TJ; Kilner MJ; Thomas EJ Synthetic approaches to phomactins: on the stereoselectivity of some [2,3]-Wittig rearrangements. *Tetrahedron* 2015, 71, 7293–7309. (aa)Du G; Bao W; Huang J; Huang S; Yue H; Yang W; Zhu L; Liang Z; Lee C-S Enantioselective Synthesis of the ABC-Tricyclic Core of Phomactin A by a  $\gamma$ -Hydroxylation Strategy. *Org. Lett* 2015, 17, 2062–2065. [PubMed: 25860178] (bb)Blackburn TJ; Thomas EJ Synthetic approaches to phomactins: Novel oxidation of homoallylic alcohols using tetra-*n*-propylammonium perruthenate. *Tetrahedron* 2018, 74, 5399–5407. (cc)Burnell ES; Irshad A-R; Lee ATL; Thomas EJ Synthetic approaches to phomactins: Late stage stereochemical and reactivity issues. *Tetrahedron* 2018, 74, 6737–6748.
- (14). Miyaoka H; Saka Y; Miura S; Yamada Y Total synthesis of phomactin D. *Tetrahedron Lett.* 1996, 37, 7107–7110.
- (15) (a). Goldring WPD; Pattenden G A total synthesis of phomactin A. *Chem. Commun* 2002, 1736–1737. (b)Diaper CM; Goldring WPD; Pattenden G A total synthesis of ( $\pm$ )-phomactin A. *Org. Biomol. Chem* 2003, 1, 3949–3956. [PubMed: 14664384]
- (16). Goldring WPD; Pattenden G Total synthesis of ( $\pm$ )-phomactin G, a platelet activating factor antagonist from the marine fungus *Phoma* sp. *Org. Biomol. Chem* 2004, 2, 466–473. [PubMed: 14770224]
- (17). Mohr PJ; Halcomb RL Total Synthesis of (+)-Phomactin A Using a B-Alkyl Suzuki Macrocyclization. *J. Am. Chem. Soc.* 2003, 125, 1712–1713. [PubMed: 12580592]
- (18). Huang J; Wu C; Wulff WD Total Synthesis of ( $\pm$ )-Phomactin B2 via an Intramolecular Cyclohexadienone Annulation of a Chromium Carbene Complex. *J. Am. Chem. Soc* 2007, 129, 13366–13367. [PubMed: 17929921]
- (19) (a). Tang Y; Cole KP; Buchanan GS; Li G; Hsung RP Total Synthesis of Phomactin A. *Org. Lett* 2009, 11, 1591–1594. [PubMed: 19260663] (b)Buchanan GS; Cole KP; Li G; Tang Y; You L-F; Hsung RP Constructing the architecturally distinctive ABD-tricycle of phomactin A through an intramolecular oxa-[3 + 3] annulation strategy. *Tetrahedron* 2011, 67, 10105–10118. [PubMed: 23750054] (c)Buchanan GS; Cole KP; Tang Y; Hsung RP Total Synthesis of ( $\pm$ )-Phomactin A. Lessons Learned from Respecting a Challenging Structural Topology. *J. Org. Chem* 2011, 76, 7027–7039. [PubMed: 21819039]
- (20). Huang J; Bao W; Huang S; Yang W; Lizhi Z; Du G; Lee C-S Formal Synthesis of (+)-Phomactin A. *Org. Lett* 2018, 20, 7466–7469. [PubMed: 30480457]
- (21). Bermejo FA; Mateos AF; Escribano AE; Lago RM; Buron LM; Lopez MR; Gonzalez RR Ti(III)-promoted cyclizations. Application to the synthesis of (E)-endo-bergamoten-12-oic acids. Moth oviposition stimulants isolated from *Lycopersicon hirsutum*. *Tetrahedron* 2006, 62, 8933–8942.
- (22). Masarwa A; Weber M; Sarpong R Selective C–C and C–H Bond Activation/Cleavage of Pinene Derivatives: Synthesis of Enantiopure Cyclohexenone Scaffolds and Mechanistic Insights. *J. Am. Chem. Soc* 2015, 137, 6327–6334. [PubMed: 25892479]
- (23). As seen in a related X-ray structure, the C4–C5 bond is the stronger, shorter bond (1.551 Å) compared to the weaker and longer C2–C5 bond (1.567 Å); see ref 22.
- (24). Previous synthetic work to construct the phomactin skeleton indicated that the macrocyclization step can be challenging and low yielding, particularly if the carbon at C1 is sp<sup>2</sup> hybridized. Macrocyclizations with substrates where C1 is sp<sup>3</sup> hybridized are often more facile, most likely due to better preorganization of the pendant functional group. For example, see ref 13f vs 15a. The sulfone alkylation strategy employed in this work was previously shown to be effective, but only if C1 was sp<sup>3</sup> hybridized; see refs 13l and 13s. We initially hypothesized that the rigid [3.1.1]bicycle would help facilitate cyclization while still maintaining sp<sup>2</sup> hybridization at C1. However, as shown in the final synthetic route (Scheme 8), this rigid bicycle was ultimately not required for successful macrocyclization.

- (25). For a review of preorganization in macrocyclization reactions, see: Martí-Centelles V; Pandey MD; Burguete MI; Luis SV Macrocyclization Reactions: The Importance of Conformational, Configurational, and Template-Induced Preorganization. *Chem. Rev* 2015, 115, 8736–8834. [PubMed: 26248133]
- (26) (a). Simmons EM; Hartwig JF Catalytic functionalization of unactivated primary C–H bonds directed by an alcohol. *Nature* 2012, 483, 70–73. [PubMed: 22382981] (b) Li B; Driess M; Hartwig JF Iridium-Catalyzed Regioselective Silylation of Secondary Alkyl C–H Bonds for the Synthesis of 1,3-Diols. *J. Am. Chem. Soc* 2014, 136, 6586–6589. [PubMed: 24734777]
- (27) (a). Nishimura T; Uemura S Palladium-Catalyzed Arylation of tert-Cyclobutanols with Aryl Bromide via C–C Bond Cleavage: New Approach for the  $\gamma$ -Arylated Ketones. *J. Am. Chem. Soc* 1999, 121, 11010–11011. (b) Weber M; Owens K; Masarwa A; Sarpong R Construction of Enantiopure Taxoid and Natural Product-like Scaffolds Using a C–C Bond Cleavage/Arylation Reaction. *Org. Lett* 2015, 17, 5432–5435. [PubMed: 26485318]
- (28). Allylic acetate 32 showed reactivity similar to that of allylic acetate 35 toward coupling reactions.
- (29). Del Valle L; Stille JK; Hegedus LS Palladium-catalyzed coupling of allylic acetates with aryl- and vinylstannanes. *J. Org. Chem* 1990, 55, 3019–3023.
- (30). Synthesized in five steps from 4-pentyn-1-ol. See Supporting Information for details.
- (31). Without the TMS group on the cyclobutanol, subjecting the macrocycle precursor to basic cyclization conditions only resulted in Grob fragmentation.
- (32) (a). Matsuda T; Makino M; Murakami M Rhodium-Catalyzed Addition/Ring-Opening Reaction of Arylboronic Acids with Cyclobutanones. *Org. Lett* 2004, 6, 1257–1259. [PubMed: 15070311] (b) Murakami M; Makino M; Ashida S; Matsuda T Construction of Carbon Frameworks through  $\beta$ -Carbon Elimination Mediated by Transition Metals. *Bull. Chem. Soc. Jpn* 2006, 79, 1315–1321. (c) Cramer N; Seiser T  $\beta$ -Carbon Elimination from Cyclobutanols: A Clean Access to Alkylrhodium Intermediates Bearing a Quaternary Stereogenic Center. *Synlett* 2011, 4, 449–460.
- (33) (a). Seiser T; Cramer N Enantioselective C–C Bond Activation of Allenyl Cyclobutanes: Access to Cyclohexenones with Quaternary Stereogenic Centers. *Angew. Chem., Int. Ed* 2008, 47, 9294–9297. (b) Seiser T; Cramer N Rhodium(I)-Catalyzed Enantioselective Activation of Cyclobutanols: Formation of Cyclohexane Derivatives with Quaternary Stereogenic Centers. *Chem. - Eur. J.* 2010, 16, 3383–3391. [PubMed: 20146275]
- (34). The  $\alpha$  C–H bond is pseudo-axial, providing good overlap between the C–H  $\sigma$ -bond and both the C–O  $\pi^*$  orbital and C–C  $\pi^*$  orbital, thus weakening the C–H bond.
- (35). See Supporting Figures 1 and 2 for details.
- (36). See Supporting Table 1 for details.
- (37). Other groups have utilized a similar aldehyde addition strategy; see refs 13z and 14.
- (38). Synthesized in five steps from 4-pentyn-1-ol. See Supporting Information for details.
- (39). See Supporting Figure 3 for details.
- (40). Formation of the cyclopropane ring of 67 is likely facilitated by close proximity of the transient carbanion to the carbonyl moiety. A related cyclopropane was observed in the reductive desulfonylation of a phomactin intermediate; see ref 13cc.
- (41). (a) For examples of cyclopropane rearrangements, see: Gibson DH; DePuy CH Cyclopropanol chemistry. *Chem. Rev* 1974, 74, 605–623. (b) Kulinkovich OG The Chemistry of Cyclopropanols. *Chem. Rev* 2003, 103, 2597–2632. [PubMed: 12848581]
- (42) (a). Nysted LN Methylenation reagent. U.S. Patent 3865848, 1975; *Chem. Abstr* 1975, 83, 10406q. (b) Lombardo L Methylenation of carbonyl compounds with  $\text{ZnCH}_2\text{Br}_2\text{TiCl}_4$ . Application to gibberellins. *Tetrahedron Lett.* 1982, 23, 4293–4296. (c) Chand HR Lombardo's Reagent. *Synlett* 2009, 15, 2545–2546.
- (43). Synthesized in five steps from 4-pentyn-1-ol. See Supporting Information and ref 13z for details.
- (44). Lipshutz BH; Miller TA Deprotection of 'sem' ethers: A convenient, general procedure. *Tetrahedron Lett.* 1989, 30, 7149–7152.
- (45). Nicolaou KC; Harrison ST Total Synthesis of Abyssomicin C and atrop-Abyssomicin C. *Angew. Chem., Int. Ed* 2006, 45, 3256–3260.
- (46). For an overview of the proposed biosynthesis of the phomactins, see ref 8. For biosynthetic studies, see: (a) Tokiwano T; Fukushi E; Endo T; Oikawa H Biosynthesis of phomactins:

- common intermediate phomactatriene and taxadiene. *Chem. Commun* 2004, 1324–1325.
- (b) Tokiwano T; Endo T; Tsukagoshi T; Goto H; Fukushi E; Oikawa H Proposed mechanism for diterpene synthases in the formation of phomactatriene and taxadiene. *Org. Biomol. Chem* 2005, 3, 2713–2722. [PubMed: 16032349]
- (c) Chow SY; Williams HJ; Pennington JD; Nanda S; Reibenspies JH; Scott AI Studies on taxadiene synthase: interception of the cyclization cascade at the verticillene stage and rearrangement to phomactatriene. *Tetrahedron* 2007, 63, 6204–6209.
- (d) Palframan MJ; Pattenden G The Verticillenes. Pivotal Intermediates in the Biosynthesis of the Taxanes and the Phomactins. *Nat. Prod. Rep* 2019, 36, 108–121. [PubMed: 29978865]
- (47). Catino AJ; Forslund RE; Doyle MP Dirhodium(II) Caprolactamate: An Exceptional Catalyst for Allylic Oxidation. *J. Am. Chem. Soc* 2004, 126, 13622–13623. [PubMed: 15493912]
- (48). Honda T; Mizutani H Regioselective Ring-Opening of 2,3-Epoxy Alcohols with Tetramethylammonium Triacetoxymethylborohydride. *Heterocycles* 1998, 48, 1753–1757.
- (49). Compound 86 was also synthesized by the Pattenden group, but was not identified as Sch 49027: Cheing JW; Goldring WPD.; Pattenden G Synthetic studies towards congeners of phomactin A. Re-examination of the structure of Sch 49028. *Chem. Commun* 2003, 22, 2788–2789.
- (50). At room temperature, the DMP oxidation of 89 primarily produced Sch 49027 (86).
- (51). For recent methodologies of C–C bond cleavage in unstrained rings, see: Xia Y; Lu G; Liu P; Dong G Catalytic activation of carbon–carbon bonds in cyclopentanones. *Nature* 2016, 539, 546–550. [PubMed: 27806379] Guo J-J; Hu A; Chen Y; Sun J; Tang H; Zuo Z Photocatalytic C–C Bond Cleavage and Amination of Cycloalkanols by Cerium(III) Chloride Complex. *Angew. Chem., Int. Ed* 2016, 55, 15319–15322. Roque JB; Kuroda Y; Göttemann LT; Sarpong R Deconstructive fluorination of cyclic amines by carbon-carbon cleavage. *Science* 2018, 361, 171–174. [PubMed: 30002251] Roque JB; Kuroda Y; Göttemann LT; Sarpong R Deconstructive diversification of cyclic amines. *Nature* 2018, 564, 244–248. [PubMed: 30382193] Hu A; Chen Y; Guo J-J; Yu N; An Q; Zuo Z Cerium-Catalyzed Formal Cycloaddition of Cycloalkanols with Alkenes through Dual Photoexcitation. *J. Am. Chem. Soc* 2018, 140, 13580–13585. [PubMed: 30289250] Zhao K; Yamashita K; Carpenter JE; Sherwood TC; Ewing WR; Cheng PTW; Knowles RR Catalytic Ring Expansions of Cyclic Alcohols Enabled by Proton-Coupled Electron Transfer. *J. Am. Chem. Soc* 2019, 141, 8752–8757. [PubMed: 31117664]



**Figure 1.** (A) A sequential bond formation strategy. (B) A strategy of bond formation followed by C–C bond cleavage to access rearranged carbocycles.

**Figure 2.**

(A) Representative members of the phomactin family of natural products. (B) Yamada's synthesis of (+)-phomactin D. (C) Pattenden's synthesis of ( $\pm$ )-phomactin A. (D) Halcomb's synthesis of (+)-phomactin A.

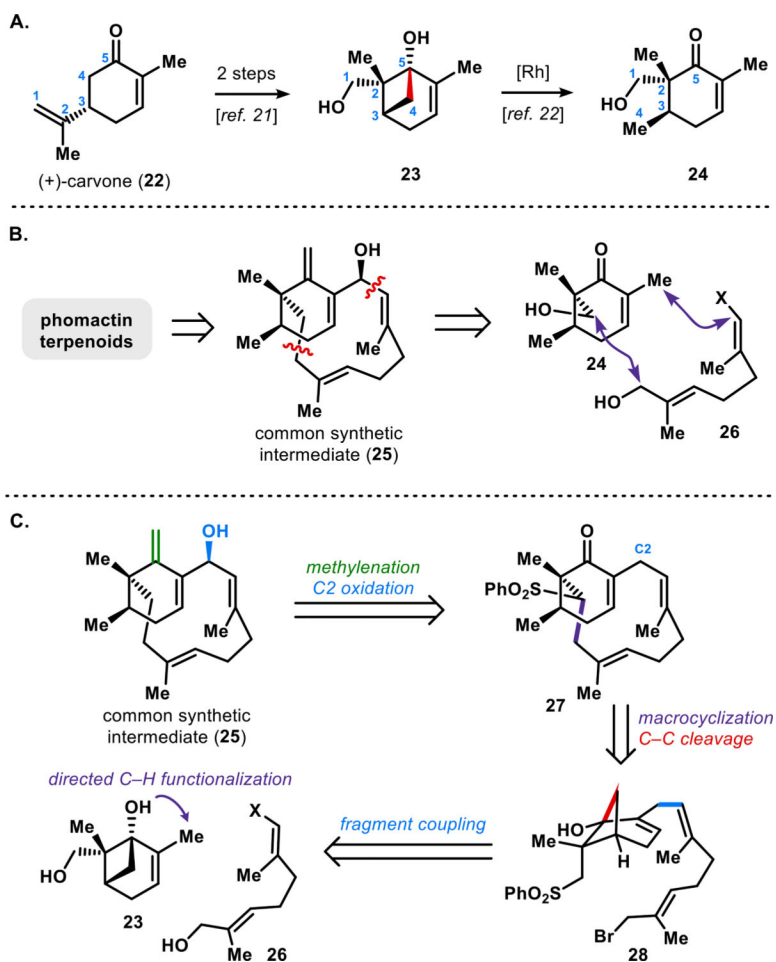
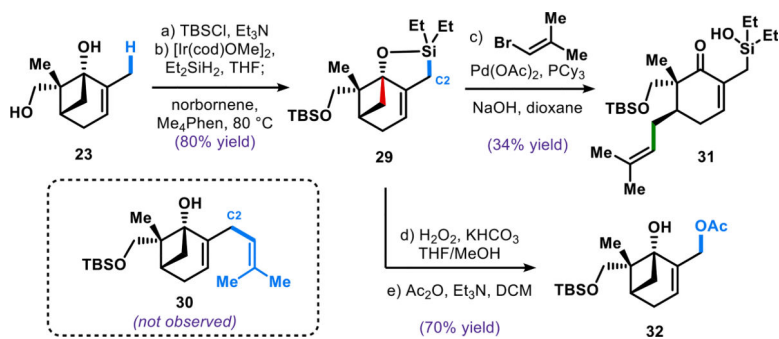
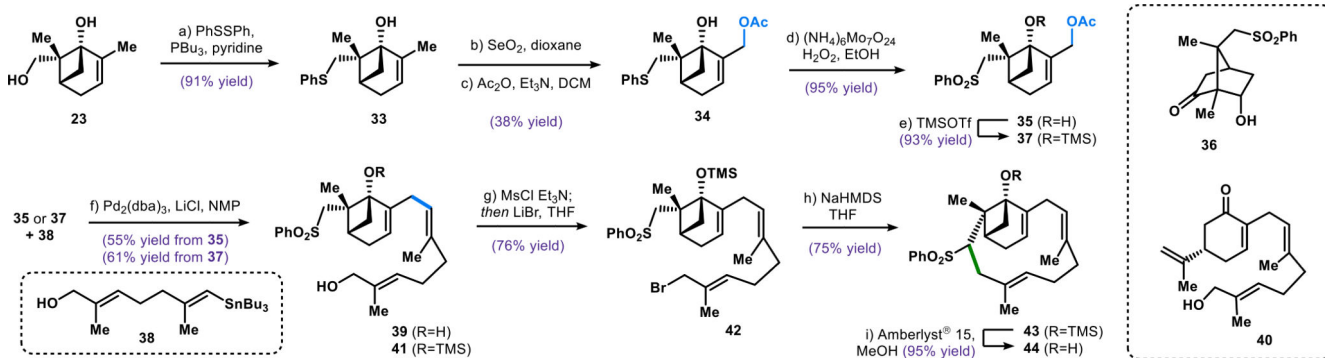


**Figure 3.** (A) Skeletal rearrangement of carvone into substituted cyclohexenone **24**. (B) Generalized synthetic strategy. (C) Initial retrosynthesis of common synthetic intermediate **25** involving delayed cyclobutanol fragmentation.

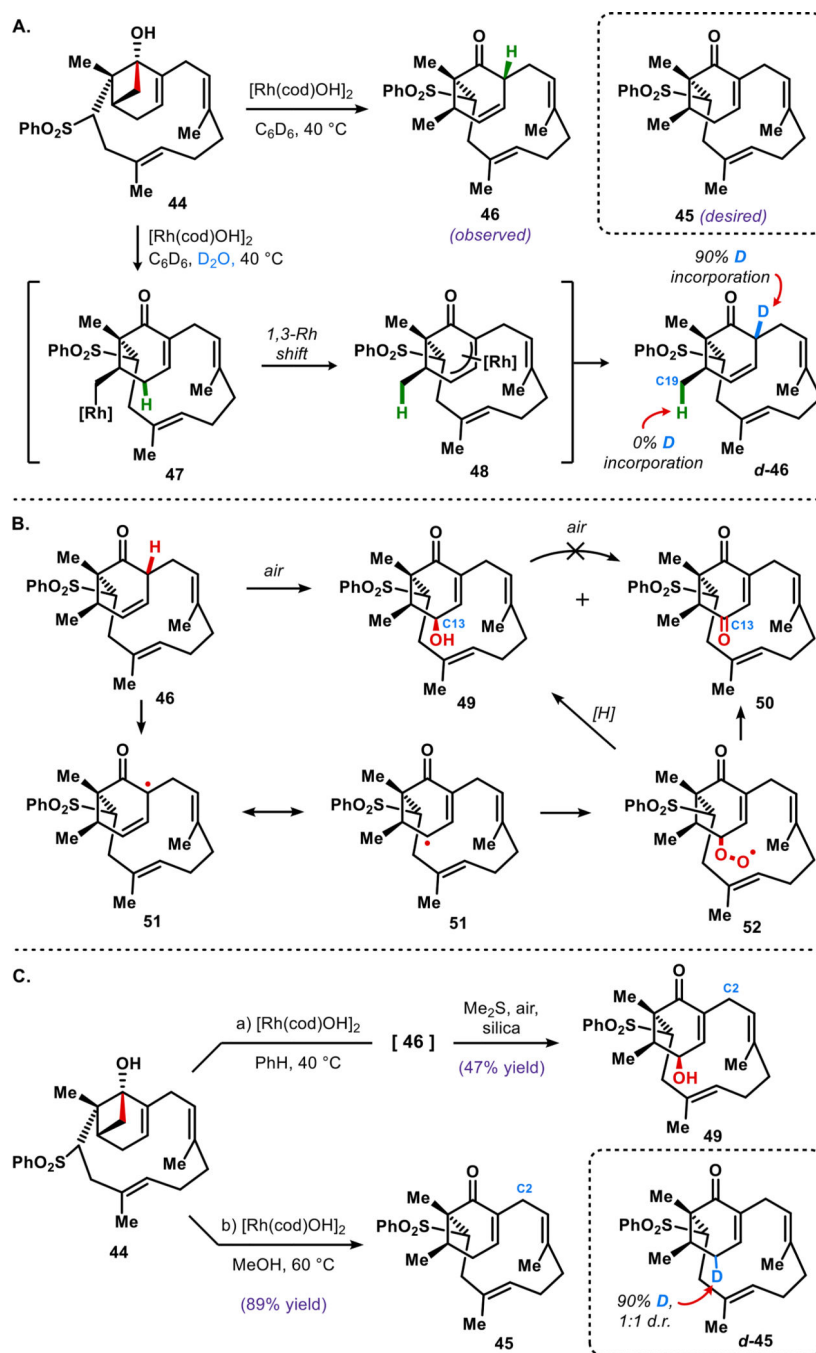


**Scheme 1.**  
Dehydrogenative C–H Silylation of Cyclobutanol 23

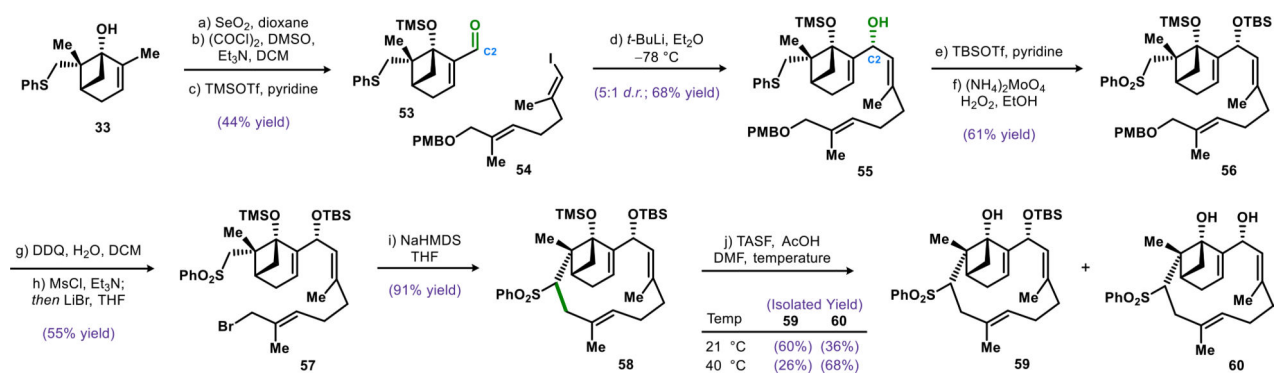




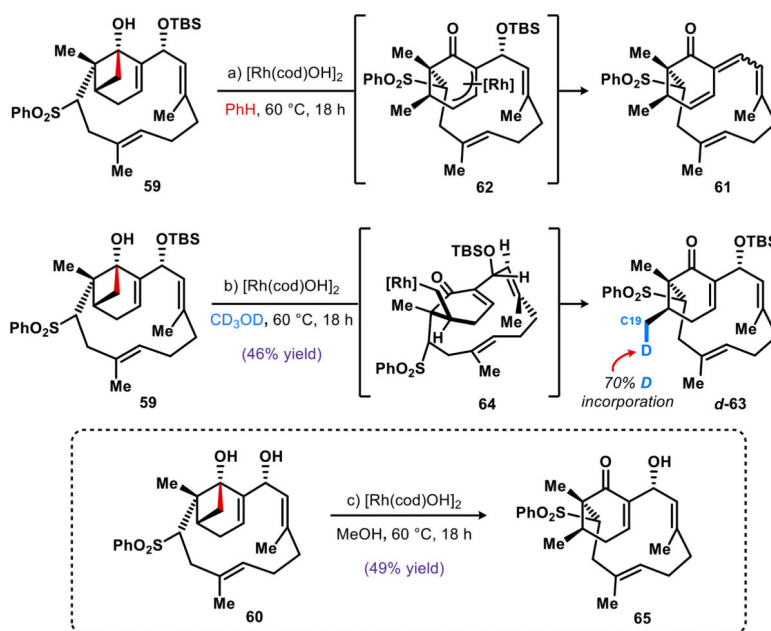
**Scheme 2.**  
Synthesis of the Macrocycle via  $\pi$ -Allyl Stille Cross-Coupling

**Scheme 3.**

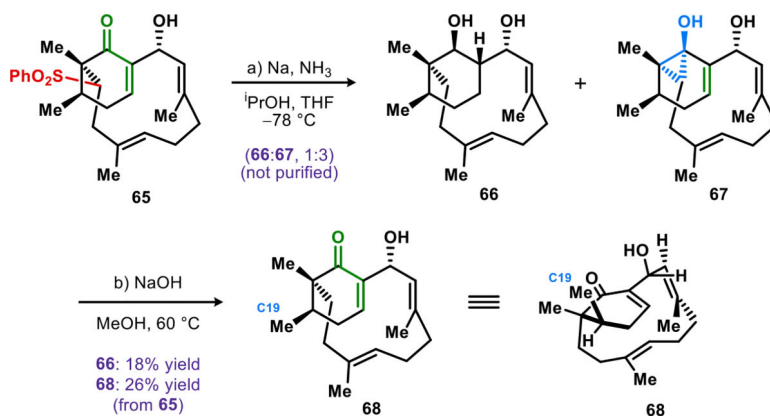
(A) Proposed Pathway for the Formation of Unconjugated Enone 46, (B) Mechanistic Hypothesis for the Formation of Oxidation Products 49 and 50, and (C) Divergent Outcomes of the Rh(I)-Catalyzed C–C Cleavage



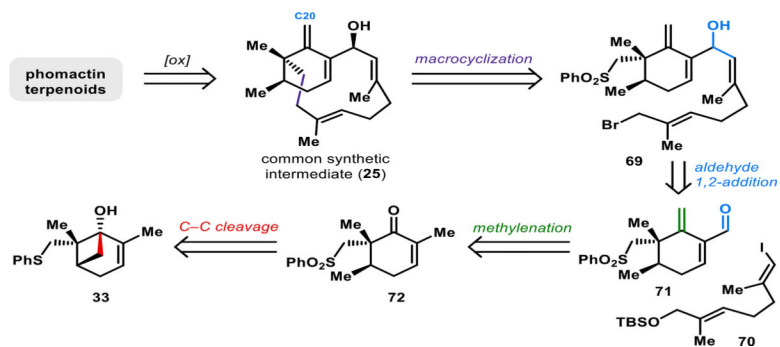
**Scheme 4.**  
 Synthesis of Macrocycle via 1,2-Addition to Aldehyde 53



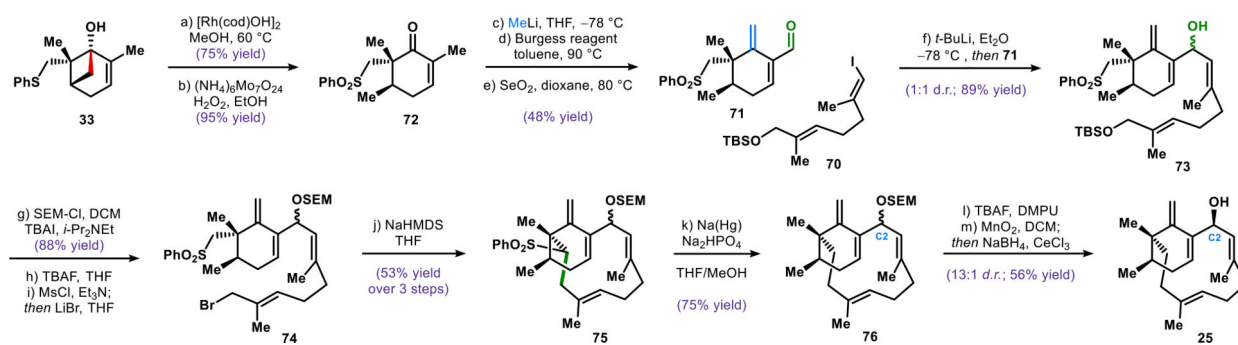
**Scheme 5.**  
Solvent Effects on the Rh(I)-Catalyzed C–C Bond Cleavage and Mechanistic Insights



**Scheme 6.**  
Reductive Sulfone Cleavage and Rearrangement of the Resulting Cyclopropanol

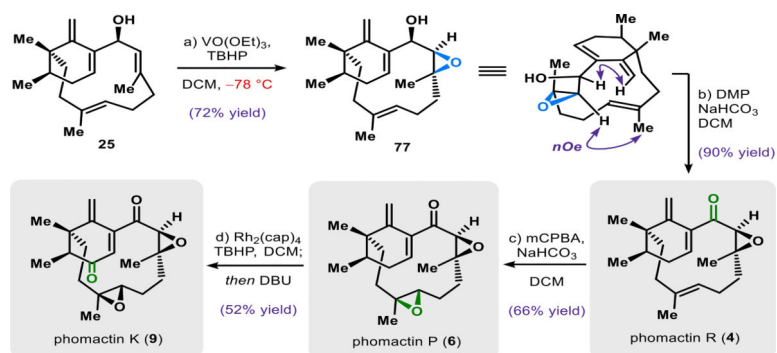


**Scheme 7.**  
Revised Retrosynthetic Analysis with Early-Stage Cyclobutanol Fragmentation

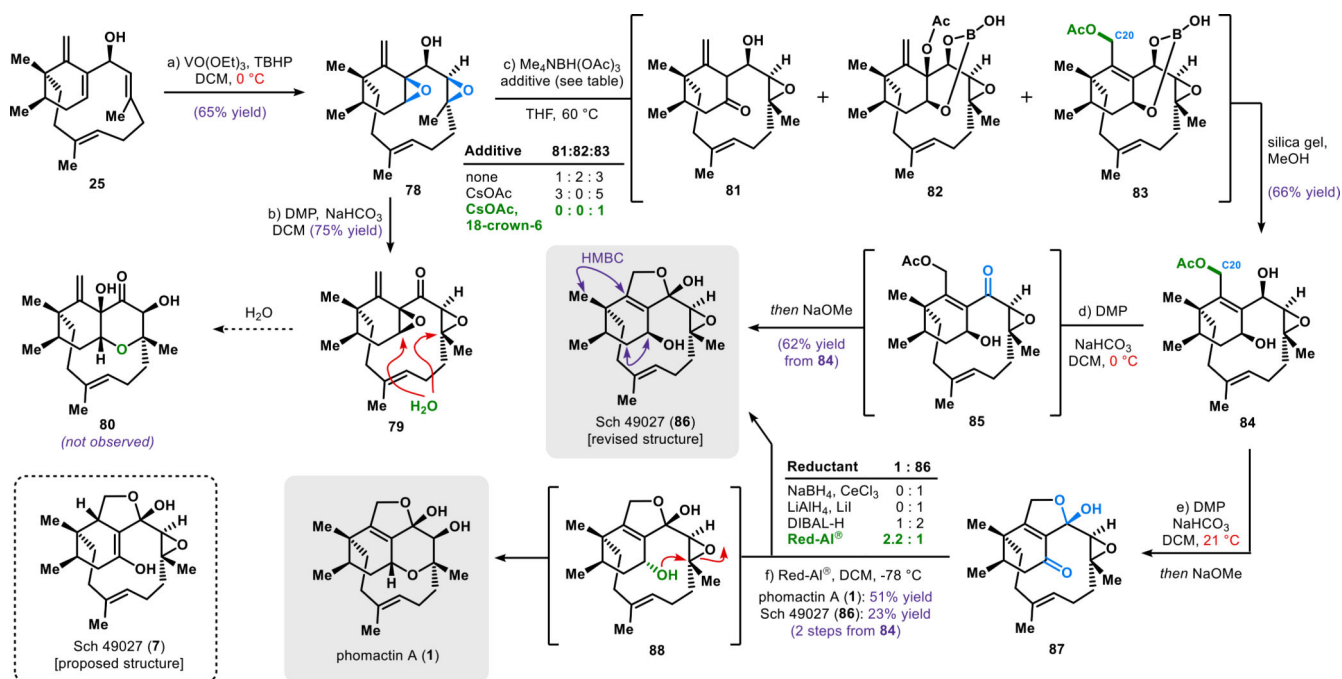


**Scheme 8.**  
Final Route to Common Intermediate 25

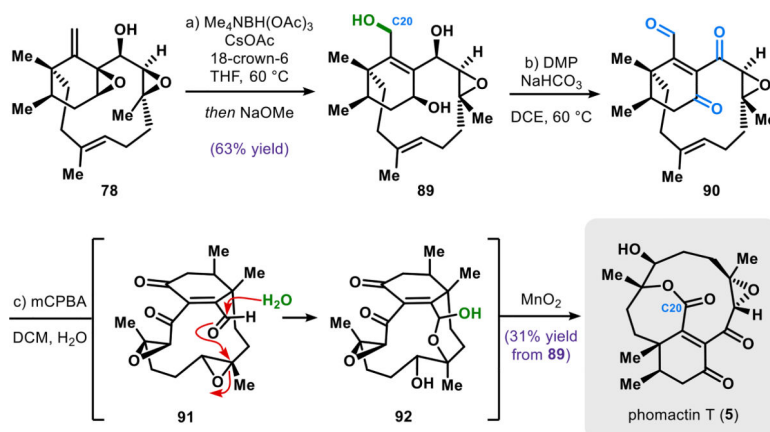




**Scheme 9.**  
Total Synthesis of Phomactins R, P, and K



**Scheme 10.**  
Total Synthesis of Phomactin A and Sch 49027 (Revised Structure)



**Scheme 11.**  
Total Synthesis of Phomactin T